AD-A070 793   OHIO STATE UNIV COLUMBUS ELECTROSCIENCE LAB   F/G 17/9
RADAR TARGET IDENTIFICATION.(U)
MAY 79   D M MOFFATT, K A SHUBERT, E M KENNAUGH   F19628-77-C-0125
UNCLASSIFIED   ESL-784677-2   RADC-TR-79-118   NL

| OF |
AD
A070793

END
DATE
FILMED
8-79
DDC

LEVEL

RADC-TR-79-118
Final Technical Report
May 1979

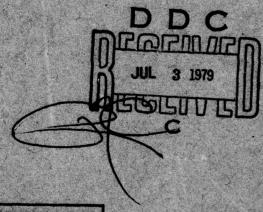# RADAR TARGET IDENTIFICATION

The Ohio State University of ElectroScience Laboratory

D. M. Moffatt
K. A. Shubert
E. M. Kennaugh

DDC
RECEIVED
JUL 3 1979
C

APPROVED FOR PUBLIC RELEASE; DISTRIBUTION UNLIMITED

ROME AIR DEVELOPMENT CENTER
Air Force Systems Command
Griffiss Air Force Base, New York 13441

79 07 02 021

This report has been reviewed by the RADC Information Office (OI) and is releasable to the National Technical Information Service (NTIS). At NTIS it will be releasable to the general public, including foreign nations.

RADC-TR-79-118 has been reviewed and is approved for publication.

APPROVED: *Otho E. Kerr*

OTHO E. KERR
Project Engineer

APPROVED: *Allan C. Schell*

ALLAN C. SCHELL
Chief, Electromagnetic Sciences Division

FOR THE COMMANDER: *John P. Huss*

JOHN P. HUSS
Acting Chief, Plans Office

If your address has changed or if you wish to be removed from the RADC mailing list, or if the addressee is no longer employed by your organization, please notify RADC (EEC) Hanscom AFB MA 01731. This will assist us in maintaining a current mailing list.

Do not return this copy. Retain or destroy.

SECURITY CLASSIFICATION OF THIS PAGE *(When Data Entered)*

REPORT DOCUMENTATION PAGE		READ INSTRUCTIONS BEFORE COMPLETING FORM
1. REPORT NUMBER RADC-TR-79-118	2. GOVT ACCESSION NO.	3. RECIPIENT'S CATALOG NUMBER
4. TITLE *(and Subtitle)* RADAR TARGET IDENTIFICATION		5. TYPE OF REPORT & PERIOD COVERED Final Technical Report. 1 Mar 77 — 30 Sep 78
		6. PERFORMING ORG. REPORT NUMBER ESL-784677-2
7. AUTHOR(s) D. M. Moffatt, K. A. Shubert, E. M. Kennaugh		8. CONTRACT OR GRANT NUMBER(s) F19628-77-C-0125
9. PERFORMING ORGANIZATION NAME AND ADDRESS The Ohio State University ElectroScience Laboratory/Dept of Electrical Engineering Columbus OH 43212		10. PROGRAM ELEMENT, PROJECT, TASK AREA & WORK UNIT NUMBERS 61102F 23050425
11. CONTROLLING OFFICE NAME AND ADDRESS Deputy for Electronic Technology (RADC/EEC) Hanscom AFB MA 01731		12. REPORT DATE May 79
		13. NUMBER OF PAGES 63
14. MONITORING AGENCY NAME & ADDRESS*(if different from Controlling Office)* Same		15. SECURITY CLASS. *(of this report)* UNCLASSIFIED
		15a. DECLASSIFICATION/DOWNGRADING SCHEDULE N/A

16. DISTRIBUTION STATEMENT *(of this Report)*

Approved for public release; distribution unlimited.

17. DISTRIBUTION STATEMENT *(of the abstract entered in Block 20, if different from Report)*

Same

18. SUPPLEMENTARY NOTES

RADC Project Engineer: Ortho E. Kerr (EEC)

19. KEY WORDS *(Continue on reverse side if necessary and identify by block number)*

Radar	Resonances
Target	Swept
Identification	Frequency
Natural	

20. ABSTRACT *(Continue on reverse side if necessary and identify by block number)*

This report presents a review of the radar target identification problem with primary emphasis on practical solutions as opposed to abstract inverse scattering formalisms. A time domain viewpoint is stressed throughout because of its compactness, ease of visualization and diagnostic potential and because it is a unifying tool for various electromagnetic approximations. A small finite set of excitation invariant target descriptors, the coefficients of a linear, homogeneous difference equation, or equivalently the complex natural

DD FORM 1473
1 JAN 73

SECURITY CLASSIFICATION OF THIS PAGE *(When Data Entered)*

(cont)

resonances, are justified as a discrimination tool. A prediction-correlation method for using these coefficients in identification is demonstrated. It is shown that substructure features of the targets, in this case vertical and horizontal stabilizers of aircraft, possibly can be used as a discrimination feature and that the required interrogating radar signal spectrum for this case is significantly higher than that required for previous discrimination schemes using excitation invariant parameters. In this specific case, however, the target parameters do not have a simple physical interpretation.

PREFACE

One need only be mildly optimistic to forecast that future generations of radar systems will routinely provide a great deal of target information beyond the usual range, elevation, azimuth and velocity. At the very least these new systems will provide parametric target data for diagnostics and the other extreme will be fully automated target identification. The key to this new sophistication will be the exploitation of broadband complex scattering data spanning several octaves. The ElectroScience Laboratory of The Ohio State University's Electrical Engineering Department has pioneered the interpretation and utilization of multiple frequency complex scattering data for numerous purposes including radar target identification. The extrapolation of these results to new generations of radar systems is the logical next step. In the interim preceding these developments it is meaningful to explore what can be accomplished if the basic broadband premise is deliberately distorted to more nearly accommodate existing radar systems. Much of the subject matter of this report is directed to this question.

iii

CONTENTS

EVALUATION

The experimental and theoretical work done on this contract shows that aircraft of similar size and/or different models of the same aircraft (examples are F104 and F104N) can be uniquely identified by processing a radar signal which contains a number of frequencies. The techniques developed use the resonances of the aircraft which are invariant with respect to the aspect angle, however their amplitude do vary with aspect. The resonances are translated into mathematical pole-zero representations for each aircraft and stored as data in a library to compare with the data received from an unknown aircraft.

This work is in support of TPO R2B. Although the frequencies used in this effort are lower than the present radars use, the technique may possibly be used at higher frequencies to detect smaller resonant parts of aircraft that are unique to each aircraft.

OTHO E. KERR
Project Engineer

INTRODUCTION

The subject matter of this report is the discrimination of radar targets; specifically aircraft targets of the jet fighter class. Discrimination* rather than identification is used here to denote that the techniques to be described distinguish targets <u>within</u> a given class. Targets not in the class can at best be categorized as being outside the class and possibly looking most like a particular target in the class. It is not intended to imply from the above that targets of disportionate size as, e.g., bombers and light aircraft, cannot be discriminated. This in fact is a simple discrimination task. Conversely, the discrimination of targets of nearly equal size and similar shape is a most difficult task. It is this difficult task which is addressed in this report.

Active radar interrogation, regardless of the particular radar system, basically involves the interaction of electromagnetic waves and material objects. From a system viewpoint the radar cross section of a target is a statistical quantity. However, to achieve an insight into the identification problem it is necessary to return to a fundamental deterministic model. The scattered electromagnetic field from an object is controlled by the parameters listed in Table I. Only the parameters at the left in Table I are at the disgression of the system designers. To achieve a target detection and identification capability therefore requires a systematic processing of selected parametric variations available to the designer. To select the appropriate parameters, however, requires a fundamental understanding of how each of the target characteristics at the right in Table I affects the scattered field. It is interesting to observe that the above remarks could just as easily be applied to radar cross section control if one interchanges the controllable and noncontrollable <u>parameters.</u>

*Hereafter the words identification and discrimination are used interchangeably.

1

Table I

Frequency	Target Size
Time	Target Shape
Radar Polarization	Target Composition
Pulse Shape and Length	Target Orientation
Pulse Repetition Frequency	Target Velocity
Source-Receiver Separation	Component Target Motion

Scattering Parameters

Radar practitioners will immediately observe that the last three
items on the right in Table I, orientation, velocity and component
motion, can and are exploited as a basis for target identification.
For example, a combination velocity pattern and heading usually in-
dicates a particular mission and consequently a particular vehicle.
Component motion such as the rotor blades on helicopters place a par-
ticular modulation on the radar signal. Other mechanisms yield modu-
lations of the signal or perturbations of the doppler spectrum. We
do not pursue such mechanisms because they are not fundamental to
the electromagnetic interactions of the basic target. That is, a
modulation induced by a small antenna on a spherical object may in-
deed be recognizable but the relationship to the basic spherical ob-
ject is secondary. By the same token, a given complex target may
exhibit particular modulation or doppler characteristics but the re-
lationship to the object is secondary. Such characteristics would
also appear to be easily camouflaged or distorted. Conversely, the
identification parameters pursued on this contract are fundamental
to either the overall physical properties of the radar targets or
a projected subset of them. The use of identification; friend, foe
or neutral (IFFN) techniques with transponders have also been ignored.
It is unlikely that unfriendly targets will be cooperative and respond
to interrogation overtures. Even friendly targets may find it unwise

2

to respond because of tactical considerations. The identification
procedures pursued on this contract do not require the cooperation
of the target.

The first three parameters at the left in Table I are the most
fundamental quantities in terms of eliciting physical properties of
the target. This insight has been achieved via the impulse response
concept[1,2] as applied to electromagnetic scattering problems. One
of the first things that became apparent was that the gross physical
properties (size, shape and composition) of the target were most in-
timately related to its scattering characteristics at low frequencies.
In fact, at the highest frequency of interest the maximum linear di-
mension of the target is only one and one-half to two wavelengths.
That is, maximum gross physical property information is contained
in this frequency range. From the viewpoint of ease of implementation
obviously higher frequencies are of interest. One must recognize
however that the use of such higher frequencies necessarily entails
some loss of fundamental identification potential. The scattering
characteristics of the target at higher frequencies are related to
isolated features of the target rather than the target as a whole.
This is the reason why approaches to the target identification problem
using modulated short pulse radars have generally failed. One indeed
isolates the flare spots by this approach but how these fit together
to form the total target is most difficult if not impossible in most
cases to answer. A bistatic angle for the radar is clearly a designer-
controlled parameter. In fact, if several receivers are employed
then tracking of the flare spot variations with target orientation
has been postulated as a modulated short pulse radar identification
process. The intent here is not to evaluate this or any other iden-
tification technique, and over the years various exotic schemes for
coded variations of the controlable parameters have been proposed.
We note however that as the class of targets to be identified grows
larger the training set for identification by this approach could
quickly become unwieldy.

3

It is customary in almost any diagnostic or identification problem to utilize all of the available observables. The approach adopted here however minimizes the parameters used to characterize the target. Each target, even for such complicated structures as aircraft, is uniquely characterized by a small finite set of numbers. These numbers are the difference coefficients of a difference equation associated with the dominant complex natural resonances of the target or (with latest research) possibly less dominant substructure resonances. In effect, the singularties in the target transfer function are modelled as simple poles and are excitation invariant. That is, the poles are independent of the orientation of the target with respect to the radar and of the polarization of the interrogating radar signal[3,4]. It follows that the difference equation and the difference coefficients have the same properties.

Processing for detection or identification consists of comparing a measured transient response from an unknown target with a calculated transient response produced using the coefficients of a known target. Several things are involved. First, the <u>measured</u> transient response is produced synthetically from multiple frequency scattering data which with substructures can perhaps be "chirp" -type signals. Second, the <u>calculated</u> transient response is obtained using a linear difference equation[5] and the coefficients of a given target. Thus the approach assumes that the poles or coefficients for a class of target shapes of interest have previously been obtained. The fact that our identification process does <u>not</u> extract resonances from the response waveform of an unknown target turns out to be a distinct advantage. The extraction of complex natural resonances from calculated or measured scattering or radiation data is neither a simple nor exact task. The resonances can be found, but procedures which empirically remove anomalous resonances must be employed. Data from a single object orientation and a fixed polarization are not sufficient. The result is that resonance extraction is not a real time process. Fortunately

4

with our identification process preparation of the target library
is a separate task and not directly part of the scheme. Therefore
our method does yield a real time capability. Note also that the
basic question is if the target response approximately satisfies a
linear, homogeneous difference equation.

THE BASICS

The impulse response concept has been detailed in a tutorial
paper[2]. For our purpose here, it suffices to note that the transform
pair

$$G(\theta,\phi,\hat{p},j\omega) = \int_{0-}^{\infty} F_I(\theta,\phi,\hat{p},t)e^{-j\omega t}dt$$

$$F_I(\theta,\phi,\hat{p},t) = \frac{1}{2\pi} \int_{-\infty}^{\infty} G(\theta,\phi,\hat{p},j\omega)e^{j+\omega t}d\omega \tag{1}$$

relate the normalized scattered field, G, from the target to the im-
pulse response waveform, F_I, of the target. The triplet θ, ϕ, $\hat{p}$
denotes the spatial and polarization dependence. Our main interest
in the past was in the ramp response waveform

$$F_R(\theta,\phi,\hat{p},t) = \frac{1}{2\pi} \int_{-\infty}^{\infty} \frac{G(\theta,\phi,\hat{p},j\omega)e^{j\omega t}d\omega}{(j\omega)^2} \quad . \tag{2}$$

In Equation (2), noting that G can at most increase as $j\omega$, it is
clear that the ramp response waveform emphasizes the low frequency
scattering characteristics of the target. It is also clear from (2)
that information on that target's gross phyical properties is con-
tained in the ramp response waveform. The diagnostic features in-
herent in the impulse response waveform of a target should not be
overlooked. At a fixed orientation and polarization, one real time-
dependent waveform sums up the scattering properties of the object
at any frequency. Via convolution, the response to any arbitrary
interrogating signal can be quickly obtained. All of the features

5

illuminated by spectral limited asymptotic and moment methods are contained in this waveform and can be separately identified. The proper testing procedure for any postulated identification scheme is via the canonical (impulse, step and ramp) response waveforms of the object. Radar imagery features, i.e., actually producing iso-metric three-dimensional pictures of the target from radar data, are most basically considered in the time domain. We will elaborate on this point later.

Using Fourier synthesis, the ramp response waveform can be approximated as:

$$F_R(t) = \frac{-2}{\pi \omega_o} \sum_{n=1}^{2N-1} \frac{|1 - (-1)^\eta|}{n^2} |G(\theta,\phi,\hat{p},jn\omega_o)| \cos(n\omega_o t + \xi(n\omega_o))$$

(3)

or as

$$F_R(t) = -\frac{1}{\pi \omega_o} \sum_{\eta=1}^{2N} \frac{|G(\theta,\phi,\hat{p},jn\omega_o)|}{n^2} \cos(n\omega_o t + \xi(n\omega_o)),$$

(4)

where

$$\xi(n\omega_o) = T_{an}^{-1} \left[\frac{\text{Im}\{G(\theta,\phi,\hat{p},jn\omega_o)\}}{\text{Re}\{G(\theta,\phi,\hat{p},jn\omega_o)\}} \right].$$

(5)

For all but the most perverse targets (those with jump discontinuities in the ramp response) an upper summation limit of eight or ten provides a good estimate of the ramp response waveform. Thus discrete scat-tering data at five odd harmonics, (3), or ten even and odd harmonics (4), suffice to determine the ramp response waveform. Strictly speak-ing, the fundamental should come from Shannon's sampling theorem but we generally will not know the effective duration of the response. The response, of course, decays exponentially but we take the effec-tive duration of the waveform to be the time to decay to roughly two percent of its peak magnitude. A general rule of thumb is that at

6

the fundamental, the maximum linear dimension of the target should be approximately one-fifth of a wavelength. The imagery possibilities follow directly from the ramp response waveform. It has been shown[2] that the magnitude of the ramp response waveform is directly proportional to the cross sectional area of the target along the line of sight, rigorously to the shadow boundary and approximately beyond. Thus image production consists of relating one or more cross sectional areas or profile functions to an object geometry[18]. This can be expressed in very elegant mathematical terms but the end result is the same. Note particularly that there is a limitation in that at certain of the interrogating frequencies the object is electrically small. Higher frequencies can obviously sharpen the image but without at least synthetic low frequency information there is no image. We stress this limitation because difference equation identification, which started with essentially the same scattering data needed for the ramp response, does appear capable of using somewhat higher frequencies alone, i.e., without the use of very low frequency information. The term "image" as used here refers specifically to a three-dimensional estimate of the target geometry obtained from an interpretation of cross sectional area (transverse to the radar line of sight) information. The cross sectional area information comes directly from the forced portion of the target's ramp response waveform. It follows that aliasing errors caused by a lack of low frequency information negate the image production unless special procedures are postulated. In any event the fundamental appears vital.

The impulse, step and ramp response waveforms of a conducting spherical scatterer for backscatter are shown in Figure 1. The waveforms shown were produced synthetically from Mie series calculations using respectively 64, 40 and 10 harmonics with a fundamental sphere circumference of 0.25 wavelengths. We repeat these waveforms in an attempt to make this report as self contained as possible. Earlier specular and creeping wave contributions are easily discernable in
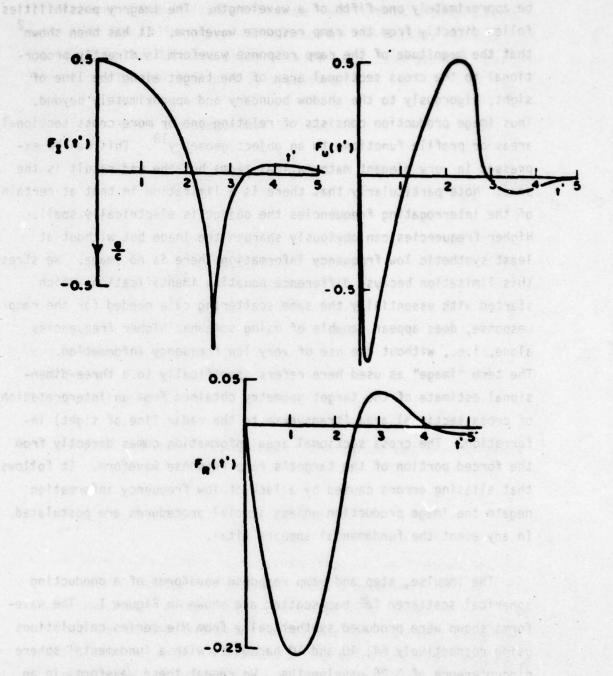
7

Figure 1. Approximate impulse, step, and ramp response waveform of conducting sphere. Backscatter.

8

the impulse response waveform as has been discussed elsewhere[2]. Note carefully that deformations of the spherical geometry beyond the shadow boundary can only alter the impulse response waveform for times greater than one delay time. This type of diagnostic potential has been little exploited in time domain studies. The ramp response waveform, shown in Figure 1 for the sphere, has been studied extensively for many targets for three principal reasons:

1) It can be produced synthetically from measurements at a very few frequencies therefore making ramp response radars feasible, if not state of the art.

2) The forced portion of the response is directly proportional to the target's cross sectional area and therefore radar imaging via ramp response radars is a demonstrated capability[13].

3) The transient portion of the ramp response can be well approximated by a finite exponential sum[2], meaning that excitation invariant dominant complex natural resonances can be used to characterize the target[8,15,17].

It is interesting to observe that an exponential sum approximation of the impulse response waveform of the sphere for transit times greater than one would appear to require many terms to approach a reasonable estimate.

LOCATION OF THE TARGET POLES

First efforts at effecting target classification via excitation invariant parameters viewed the dominant complex natural resonance (poles) as the fundamental elements. In fact, recent studies on Prony's method and its variations continue to view the poles as the desired end result. It now appears that a more meaningful characterization should perhaps be couched in terms of the difference coefficients

9

of a linear difference equation. The reason for this and the relation-
ship between the poles and difference coefficients will be discussed
later. In the following we first describe the methods and procedures
for locating the dominant poles of a target. Subsequently, the dif-
ference coefficient approach is discussed.

If one makes the approximation that

$$F_R(\theta,\phi,\hat{p},t) = \sum_{n=1}^{N} A_n(\theta,\phi,\hat{p})e^{\delta_n t}, \tag{6}$$

or equivalently

$$G(\theta,\phi,\hat{p},j\omega) = \frac{\sum_{r=1}^{Q-1} C_r(\theta,\phi,p)(j\omega)^r}{\sum_{q=0}^{Q} D_q(j\omega)^q}, \tag{7}$$

then in Equation (6),

$$\delta_n = -\sigma_n \pm j^{\omega_n}, \tag{8}$$

are the complex natural resonances of the target and are the roots
of

$$\sum_{q=0}^{Q} D_q(j\omega)^q = 0 . \tag{9}$$

What we have in fact done is to assume that at low frequencies the
electromagnetic scattering problem, truly a problem involving a dis-
tributed parameter system, can be modelled as a lumped circuit. We
note that the concept expressed in (6) and (7) was first suggested
in 1965[2], several years in advance of the so-called singularity ex-
pansion method[6]. We stress again the approximation involved.

10

For spheres and infinite circular cylinders, the poles can be obtained via solutions of transcendental equations, given by Stratton[7] for spherical targets. For an arbitrary target geometry other techniques must be utilized. The first attempt to locate the dominant poles of an arbitrary structure was by rational function fits (7) of calculated or measured multiple real-frequency scattering data. That is, a system of simultaenous linear equations

$$G(\vartheta,\phi,\hat{p},j\omega_i)\left[1 + \sum_{q=1}^{Q} D_q(j\omega_i)^q\right] + \sum_{r=1}^{Q-1} C_r(\theta,\phi,\hat{p})(j\omega_i)^r \qquad (10)$$

was solved for the D_q and C_r coefficients and then the roots of the polynomials were extracted. Equation (10) was applied to various target orientations to test the excitation invariance of the poles[3]. It was found that while the poles did not display the precise invariance predicted, the results were sufficiently successful to warrant further study. The rational approximant approach was temporarily abandoned with the advent of an iterative search procedure applied to an integral equation formulation of the scattering or radiation problem[3,6].

Details of a reaction integral equation formulation for the radiation or scattering by thin-wire structures have been given[9]. For arbitrary wire structures it is somewhat simpler to obtain the poles using a radiation approach. It should be understood that one must assure that all of the dominant poles of the structure have been excited. This is done by using several asymmetrically located generators on the structure. The integral equation is reduced to the finite matrix equation

$$[Z(s)][I(s)] = [V(s)] . \qquad (11)$$

$Z(s)$ is an $\eta \times \eta$ open circuit impedance matrix whose size is dictated by the number of wire segments used, $[I(s)]$ and $[V(s)]$ are current

11

and voltage column vectors and (s) is complex frequency. Formally, the poles are given by the solutions of

$$|[Z(s)]| = 0. \tag{12}$$

Numerically it is somewhat simpler to find the peak magnitude of the admittance $Y(s)$ at the generator terminals. If s_1 is a complex frequency starting point then

$$s = s_1 - \frac{Z(s_1)}{\left.\frac{Z(s)}{s}\right|_{s = s_1}} \tag{13}$$

is applied iteratively ($s - s_1$ a small step) until further changes do not occur. The numerical search procedure is attractive in the sense that it will, when applied correctly, always lead to a set of poles. However, it has some serious disadvantages. Modelling of the target structure by a wire grid configuration can become quite elaborate for complex structures such as aircraft[9]. Calculations at complex frequencies using Richmond's program[10] are normally quite efficient but the iterative search procedure is horrendously inefficient. If more than just the dominant poles are needed, the problems are magnified because more wire segments are needed to model the target at higher real frequencies. At this time there is also an upper frequency limit based on the electrical size of the structure.

A third method of locating the poles utilizes what is known as Prony's method[11,4]. Prony's method linearizes the process of obtaining an approximate fit of a waveform by a finite sum of exponentials (Equation (6)), and is adequately explained in the literature. A less restrictive method, termed an eigenanalysis solution[19], can also be applied. Both can be explained as an N term difference equation fit to sampled (Δt) data yielding

12

$$\sum_{n=1}^{N} x_n f(t_m - n\Delta t) = \epsilon_m,$$

$$m = 1, 2, \ldots M. \tag{14}$$

where ϵ_m a minimum is desired. This can be put in a quadradic form as

$$\sum_{m=1}^{M} \epsilon_m^2 = [\tilde{x}] \, [A] \, [x] , \tag{15}$$

where $[A]$ is a symmetric square matrix (NxN) and

$$a_{jk} = a_{kj} = \sum_{m=1}^{M} f_j(t_m - k\Delta t) f_k(t_m - j\Delta t) . \tag{16}$$

The Prony and eigenanalysis methods are two ways for finding the components of $[x]$. With the Prony method, the x_o coefficient is set to unity and the squared error minimum obtained with this constraint. The eigenanalysis approach chooses the components of $[x]$ as those of the eigenvector of the minimum eigenvalue of the symmetric matrix $|A|$. The two methods lead to different squared errors[19], indicating that the constraint imposed in the Prony approach is real, i.e., some generality is lost. It has recently been shown[25] that there are really N+2 least squared error solutions for the coefficients if interpolation methods are included.

The Prony and eigenanalysis methods have the advantage that they can be applied to either measured or calculated transient response waveforms. Our normal procedure has been to obtain a ramp response waveform via Fourier systhesis using (3) or (4) and either calculated or measured data. Both methods, however, do have some problems. It is necessary to apply them over different later (after the excitation is gone) time portions of the waveform until a best fit is obtained. It does not necessarily follow that the poles obtained

13

via these methods will be the same as those obtained using the integral equation approach. An example of this will be given in another section of the text. Both methods yield almost amazingly good fits to the intermediate and late time portions of transient signals but no physics is associated with the algorithm. Thus, occasionally, right half-plane poles crop up as do poles which give an excellent fit to the waveform but are anomalous. When the target orientation and radar polarization are such that a pole is only very weakly excited, the methods seem to extract the imaginary part of the pole correctly but large errors can occur in the real part. This also occurs when the data are noisy[19]. It is our experience that best results are obtained using the methods when all of the desired poles are extracted simultaneously. Procedures which suggest systematically working toward earlier times, i.e., increasing the time span covered and correspondingly increasing the number of poles extracted may work well with ideal data but are not effective for real world data where the errors are cumulative.

Recently the rational approximant approach to target pole locations has been applied to admittance calculations at real and complex frequencies. That is, the region of the complex frequency plane of interest is spanned by a regular grid of frequencies. The data were then utilized as described by (10) and the subsequent discussion. As could be anticipated, poles extracted via this approach were in very good agreement with those previously obtained via interactive search or the Prony and eigenanalysis methods[12]. The improvement over results previously obtained using only real-frequency data was dramatic. This approach to target pole extraction has two principal disadvantages. First, it is not applicable to measured data and second, for a target whose poles are completely unknown, the required density of complex frequency calculations may preclude use of the method on complicated target structures. In any event, the calculations will have to be computationally efficient.

14

EXAMPLES OF DOMINANT TARGET POLES

In this section we will present dominant target poles for a number of structures, both simple and complex. Examples will be given of poles found by certain of the methods discussed in the previous section. We concern ourselves here with relationships which can be found between the target size and shape and the pole locations. The reader should note that in every case only the second quadrant poles are shown. There are of course complex conjugate poles in the third quadrant. Also, the poles are plotted in the complex wavenumber length plane and sometimes with an additional pi normalization.

Figure 2 shows the first four dominant pole loci of a thin wire (length to diameter ratio 0.002) as it is bent about its midpoint. The resonance at lowest frequency in Figure 2 is identified as the first even resonance because at this frequency the current distribution on the wire is even with respect to the center of the wire with no current nulls except at the endpoints of the wire. For the first four modes the current distributions resemble respectively one-half cosine, one cycle sine, one and one-half cycle cosine and two cycle sine. With this in mind one can anticipate that as the wire is bent nearly double the even modes will migrate to the imaginary axis to become nonradiating or energy storage modes because they cannot exist on a wire one-half the length of the original wire. This is seen in the loci of Figure 2. Conversely, the odd modes will migrate to take up new positions as respectively first even and first odd modes on the new wire length. These loci terminations are shown as crosses in Figure 2. There is one additional lesson to be learned from Figure 2. Proximity of the pole to the imaginary axis does not necessarily indicate a strong resonance, one must also know the residue of the pole.
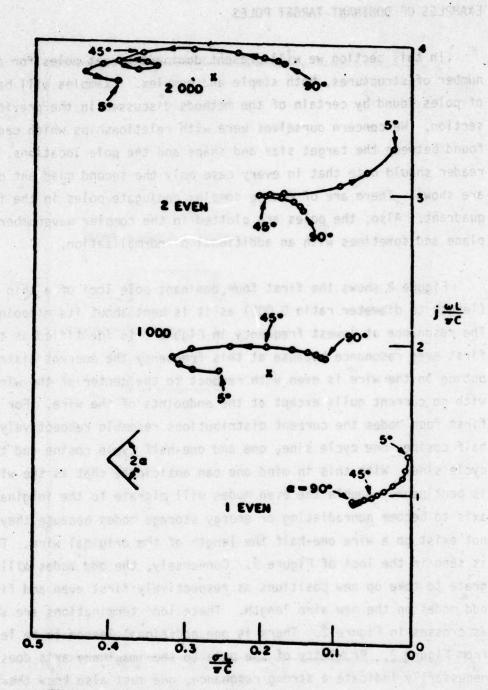
15

Figure 2. Natural resonances of bent wire with variable
included angle.

The loci shown in Figure 2 were found using the iterative search procedure with one or more generators located at asymmetrical points on the wire. As we progress to more complex structures, several generator locations will have to be used in an attempt to locate <u>all</u> of the dominant poles. With the simplified search procedure described in the previous section there is no way to guarantee that all the poles have been found. One could of course use Cauchy's residue theorem by systematically numerically integrating around contours in the complex plane but this would be expensive and time consuming and the search procedure is already inefficient. As will be seen later, one can usually detect an absent pole by applying the discrimination test for several target orientations.

Figures 3 and 4 show the poles of two perpendicularly crossed wires. In Figure 3 the wires are crossed at their centers and in Figure 4 they are crossed at one-third the length of one wire. The pole nearest the imaginary axis in Figures 3 and 4 corresponds to a bent or L-type current mode on the wires. The poles in Figures 2 ($\alpha = 90^\circ$), 3 and 4 show a reassuring self-consistency in that the poles corresponding to the first and second even modes are undisturbed, as should be the case. The poles in Figures 3 and 4 were also found using the interative search procedure. The poles of two simple stick models of straight and swept wing aircraft are shown respectively in Figures 5 and 6. Again, the interative search procedure was used to find the poles indicated by circles. The poles shown as crosses will be discussed shortly. Note here however that only one pole is significantly different for the two aircraft. We shall return to this point later.

The dominant poles of a conducting circular thin disk of radius a are shown in Figure 7. These poles were found by a method suggested by Berni[13], which is essentially equivalent to Prony's method. The poles were extracted from transient waveforms produced synthetically from calculated frequency domain scattering data[14]. The results in
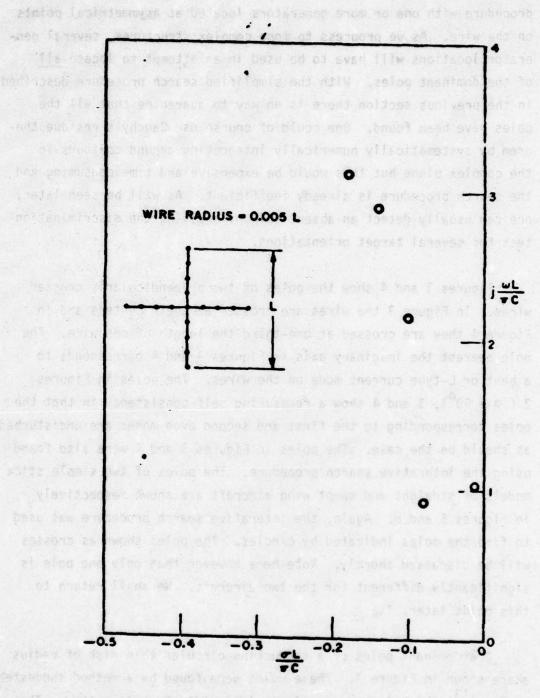
17

WIRE RADIUS = 0.005 L

$j\dfrac{\omega L}{\pi C}$

$\dfrac{\sigma L}{\pi C}$

-0.5   -0.4   -0.3   -0.2   -0.1   0

Figure 3. Natural resonances of mutually bisecting thin wires.
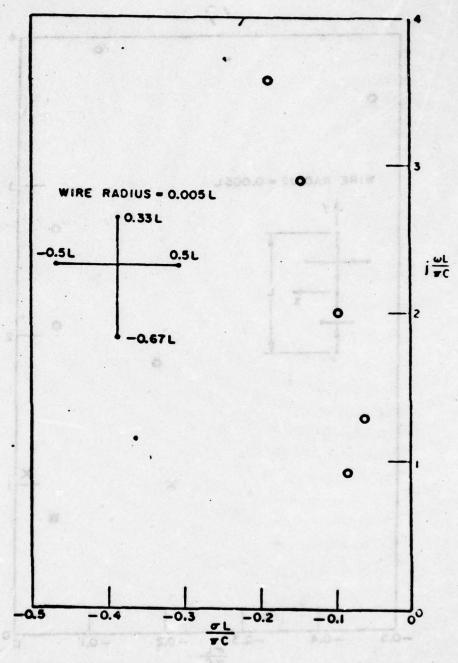
Figure 4. Natural resonances of off-center crossed
wire structure.
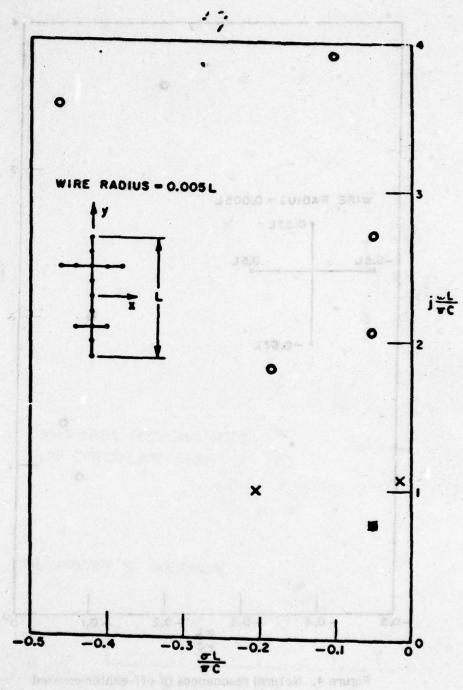
19

WIRE RADIUS = 0.005L
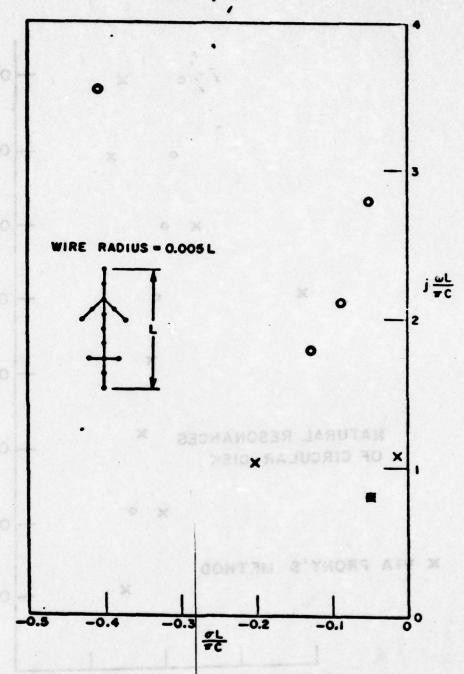

Figure 5. Natural resonances of straight wing
aircraft model.

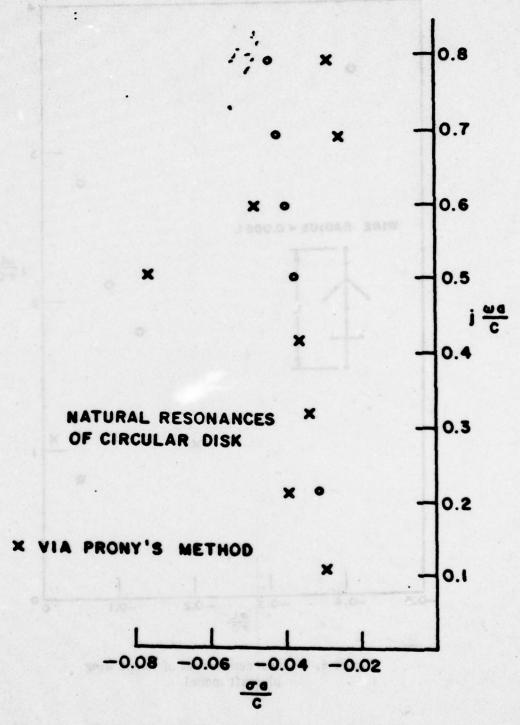Figure 6. Natural resonances of swept wing aircraft model.

Figure 7. Complex natural resonances of a thin
circular disk.

Figure 7 show one basic weakness of the Prony method. The poles shown as crossed are the actual poles found. However, for the regular disk geometry one would anticipate a string of poles similar to those for a wire or sphere. The imaginary part of the poles show this type of behavior but certain of the real parts do not. The proper locations for these poles are indicated by circles. That these positions were correct was confirmed by comparing transients calculated using · the poles to the transients obtained synthetically from the calculated frequency domain data. It has been our experience that when the Prony method fails it first yields incorrect real parts for the extracted poles. The Prony results in Figures 5 and 6, which differ from the interative search poles except for one pole, were not the result of failure of the Prony method. In this particular case the frequency domain scattering data used to synthesize the transient response only spanned $\omega L/\pi C = 0.1 \ (0.1)1.0$. Clearly the frequencies were much too low to excite the other poles found via interative search. This does illustrate another type of difficulty with the Prony method. The number of poles to be extracted must be specified, and it is not always clear from the residues which poles are anomalous.

The dominant pole locations for eight aircraft have been given[20]. These poles were obtained via Prony's method applied to transient scattered waveforms from the aircraft. It is emphasized that the transient waveforms were produced from good electromagnetic models of the aircraft[9]. That is, calculated backscatter data agreed well with experimental model measurements. To date, most of the identification studies using predictor-correlator processing has concentrated on the F-4, F-104 and MIG-19 aircraft. The poles for these targets are given in Table II.

23

TABLE II

Aircraft	$\sigma(\times 10^{-6})$	$j\omega \times 10^{-6}$
F-104	-19.7	± 94.00
	- 7.01	± 46.8
	- 3.5	±131.0
F-4	-16.4	± 66.0
	-10.9	± 43.7
	- 9.9	±130.0
MIG-19	- 8.72	± 79.3
	- 6.56	± 55.6
	- 9.35	± 66.2
	- 2.40	±130.0

Dominant Natural Resonances of F-104, F-4
and MIG-19 Aircraft.

It should be noted in passing that once the complex natural resonances of a class of targets are known, there are a number of ways one might postulate exploiting them for identification. Note however that with present resonance extraction methods it is not feasible to suggest real time extraction of the resonances from a signal obtained from an unknown target. Using the impulse response, the response to an arbitrary interrogating signal, $E^i(t)$ is

$$F^S(t) = \int_0^\infty F_I(t-\tau)E^i(\tau)d\tau \qquad (17)$$

A method of rapidly calculating this convolution has been given[2]. To visualize the possibilities, approximate the impulse response as an infinite summation, then

$$F^S(t) = \sum_{n=1}^{\infty} A_n \int_0^{\infty} e^{\gamma_n(t-\tau)} E^i(\tau) d\tau .$$ (18)

If certain of the resonances (γ_n) are known then various forms of the interrogating signal might be used to exploit this knowledge. This is perhaps best seen in the frequency domain recalling that only a finite number of poles need be excited

$$\mathscr{L}[F^S(t)] = \sum_{n=1}^{\infty} \frac{A_n}{s + \gamma_n} \mathscr{L}[E^i(t)]$$ (19)

SUBSTRUCTURE COMPLEX NATURAL RESONANCES

It has long been recognized that a major problem associated with the successfully demonstrated dominant complex natural resonance approach to identification developed at this laboratory is the spectral radar data required. The requirement of multiple frequency complex coherent radar data, while severe, is within the state of the art. Moreover, it has been shown that certain of the frequencies and phases can be deleted[3]. However, the fact that the required sampling frequencies are low, e.g., roughly 2.0 to 20.0 MHz for fighter-type aircraft, is much more difficult to circumvent. There are obvious beamwidth and other problems although it should be noted that if a long range capability were sought these frequencies for an over the horizon system are not unrealistic. In this case there are other problems such as coherency for the bounce path which would require study. In any event it is doubtful that an airbourne identification radar which exploits dominant complex natural resonances of targets is feasible

25

except on large airframes unless a synthetic aperture approach were employed. For this reason methods have been sought whereby the exploitation of target complex natural resonances for identification is retained but the required interrogation frequencies are raised significantly.

Any finite three-dimensional object has an infinite number of singularities in its transfer function, i.e., that function which transforms the incident field into the scattered field at a great distance from the object. Thus in principle there are an infinite number of complex natural resonances (it does not necessarily follow that all of these singularities can be modeled as poles of some finite order). These resonances are basically of two types if we view the second quadrant of the complex frequency plane as horizontal layers bounded by zero and some constant values of oscillatory frequency. There are 1) multiples of the dominant complex natural resonances and, as the upper bound (nonzero constant $j\omega$) increases, 2) the beginning of new strings of resonances as smaller geometrical features of the object reach complex resonance proportions. If the layers (two constant values of $j\omega$) are thought of as strips of constant width then it follows that the density of resonance locations within a strip increases as $j\omega$ increases. A primary objective of this research program was to determine if target identification could be achieved using complex natural resonances associated with smaller geometric features of the object. This choice as opposed to multiple resonances was made because it is known that multiples of a dominant resonance have an ever-increasing damping with respect to multiplicity, i.e., the resonances become like low-Q structures.

For aircraft the two most logical substructure resonance features are combinations of the vertical and horizontal tail stabilizers and the intake cavities of the jet engines. In this research program both features have been studied. The approach is experimental because

26

detailed computations which must necessarily include the influence
of the supporting airframe would be a study in itself. Even experi-
mentally the study is complicated by the fact that for these features
estimates of the appropriate spectral region where the feature will
be most influential are most difficult. This is particularly true
for the stabilizers since both (horizontal and vertical) must be con-
sidered as supporting certain basic modes. The philosophy behind
the measurement program and the results of that measurement program
are given in a separate report[24]. For six 1/72 scale models of fighter
aircraft and one pencil-type model containing a vertical stabilizer
and a shorted cavity, swept frequency amplitude and phase measure-
ments were made in appropriate spectral ranges. From these data syn-
thetic pulse response waveforms were generated. From these results
it is possible to conclude that for certain aircraft both the sug-
gested substructure features have at least partially dominating in-
fluence in the approximate full scale range of 28.0 to 100 MHz. How-
ever, a high-Q type resonance effect was _not_ observed. The processing
of these data and the results are reported here. The basic question
now being if an excitation invariant linear, homogeneous difference
equation can be found for at least one target, the implication being
others can be similarly treated.

A final point needs to be made, particularly since only very
limited results are reported. The _basic_ interrogating frequency range
for identification continues to be that span where the maximum linear
dimension of the target is at most a wavelength. It is this span
of frequencies which elicit the fundamental physical properties of
the target. It follows therefore that if the interrogating frequencies
are raised above the fundamental span as is suggested here, one can
anticipate a possible corresponding degradation in target identification
results. Identification results using measured noisy data in the
fundamental range were excellent[4]. Therefore good identification
may still be possible using substructure features but some possible

27

loss of potential may ensue. As noted earlier, it was found experimentally[24] that a response from the tail region dominated the return from the aircraft in the 30.0 to 56.0 MHz region but the characteristics of a high-Q resonance were not observed. In many cases only a single reflected pulse is seen. We seek here to use the envelope of this pulse response beyond the peak of the pulse to characterize the target via a difference equation. It follows that "poles" obtained from the resulting difference coefficients will not have a physical interpretation in terms of the stabilizers. This, however, does not preclude using the coefficients for identification.

PROCESSING*

With the type of analysis involved, the basis question is if a portion of a discretized transient record approximately satisfies a linear homogeneous difference equation

$$\sum_{n=0}^{N} f_{N+m-n} a_n = \epsilon_m,$$

$$; \quad m=0,1,2,\ldots M; \quad M+1 \geq N+1 . \tag{20}$$

where

$$f_i = f(i\Delta t) \tag{21}$$

are the data samples taken at the sample interval Δt. The ϵ_m are the errors, assumed small, and the a_n are the unknown coefficients. The equations in (20) can be put in matrix form as

$$(F)(A) = (\epsilon), \tag{22}$$

---

*Certain of the ideas summarized here were obtained from research on another program[25].

where (F) is an $(M+1) \times (N+1)$ data matrix, (A) an $N+1$ component column vector and (ϵ) an $M+1$ component error vector. The total squared error is

$$E_M^N = (\epsilon)^T(\epsilon) \tag{23}$$

where $(\epsilon)^T$ denotes transpose. The total squared error is

$$E_M^N = (A)^T(F)^T(F)(A), \tag{24}$$

where the right side of (24) is a standard quadratic form. Define

$$(R) = (F)^T(F), \tag{25}$$

then

$$E_M^N = (A)^T(R)(A), \tag{26}$$

where (R) is a real symmetric $(N+1) \times (N+1)$ matrix. There are $N+2$ <u>different</u> minimum total squared error solutions for the coefficients. The most general in that it imposed no restrictions on any <u>one</u> of the coefficients is that of eigenanalysis[19]. Since (R) is real and symmetric

$$E_M^N = (A)^T(P)^T(\Lambda)(P)(A), \tag{27}$$

where (Λ) is a diagonal matrix of the eigenvalues of (Λ). Then with the transformation

$$(Y) = (P)(A), \tag{28}$$

and

$$E_M^N = (Y)^T(\Lambda)(Y). \tag{29}$$

29

With the restriction

$$||\Lambda|| = 1,$$ (30)

The eigenvalues, N+1 in number, are minimum squared errors and the minimum eigenvalue is the minimum squared error. The remaining eigenvalues are minimum squared errors with additional (in addition to (30)) constraints in terms of inner products of the associated eigenvectors. The eigenanalysis approach was also formulated in the z-transform domain. Based on this a general optimization procedure was tested on another program[19]. Despite the fact that a z domain approach seems ideal for discrete data, no particular advantage could be found with this method. Accordingly, further study of z-domain methods are abandoned. The roots of the characteristic equation obtained from the coefficients are excitation invariant and it follows that the coefficients are excitation invariant. This suggests that data records corresponding to several aspects and/or polarizations for a given target can be combined. Assume that we have

$$q = 1, 2, \ldots 0,$$ (31)

targets and for each target we have

$$\ell = 1, 2, \ldots L^*,$$ (32)

records, For each record and target a real symmetric matrix

$$(R_q^{(\ell)}) = (F_q^{(\ell)})^T (F_q^{(\ell)}),$$ (33)

___
*Clearly in general $L = L_q$ and $M = M_q$.

30

is obtained. Now define

$$(R_q^{(L)}) = \sum_{\ell=1}^{L} (R_q^{(\ell)}) ,$$ (34)

and (R_q^L) can be used for (R) in (26). Since the individual records
can have different effective S/N ratios a weighting of the $R_q^{(\ell)}$ is
also possible. This modified eigenanalysis approach has been used
for the data obtained on this contract.

The remaining N+1 methods for finding the coefficients consist
of normalizing (26) by one of the coefficients

$$\frac{E_M^N}{a_v^2} = \frac{1}{a_v} (A)^T (R)(A) \frac{1}{a_v} ,$$ (35)

where v is an integer (see (20)) and

$$0 \leq v \leq N ,$$ (36)

Then

$$\delta \frac{E_M^N/a_v^2}{\partial a_j} = 0, \quad j \neq v$$ (37)

is used to obtain the normal equations. For example, for Prony's
method (20) becomes

$$F_{N+m} + \sum_{n=1}^{N} f_{N+m-n} \frac{a_n}{a_0} = \frac{\varepsilon_m}{a_0} ,$$ (38)

$$m = 0, 1, \ldots M$$

where the normalization by a_0 is usually absorbed. In general

$$f_{N+m-v} + \sum_{\substack{n=0 \\ n \neq v}}^{N} f_{N+m-n} \frac{a_n}{a_v} = \frac{\varepsilon_m}{a_v}$$

$$m = 0, 1, 2, \ldots M.$$ (39)

31

For proper v, the squared error obtained with Prony's method can be reduced by almost a factor of ten. A general v approach is being studied on another program[26]. The general v approach was suggested however because of identification using prediction-correlation. Assume Prony's method is used to find the coefficients and one has

$$f_{N+m} + \sum_{n=1}^{N} f_{N+m-n} \tilde{a}_n = 0,$$

(40)

where the normalization has been absorbed and zero error now assumed. With the coefficients known, (40) is a predictor, i.e., f_{N+m} can be predicted from N previous samples. But if the samples are noisy then (40) should not be used as is because low S/N samples can be multiplied by large numbers (coefficients). Instead if a_y is the largest coefficient then (40) is normalized as

$$\frac{f_{N+m}}{\tilde{a}_y} + f_{N+m-y} + \sum_{\substack{n=1 \\ n \neq y}}^{N} f_{N+m-n} \frac{\tilde{a}_n}{\tilde{a}_y} = 0.$$

(41)

The predictor equation becomes

$$f_{N+m-y} = - \frac{f_{N+m}}{a_y} - \sum_{\substack{n=1 \\ n \neq y}}^{N} f_{N+m-n} \frac{\tilde{a}_n}{\tilde{a}_y} .$$

(42)

Now note that in general (42) is an interpolation, i.e., f_{N+n-y} comes from both prior and future samples. The equivalent expression if the coefficients are found by eigenanalysis is

$$f_{N-y} = - \sum_{\substack{n=0 \\ n \neq y}}^{N} f_{N-n} \frac{a_n}{a_y} .$$

(43)

In both (42) and (43), all of the coefficients multiplying noisy data have been reduced in magnitude. The next section of this report discusses the general identification problem.

32

IDENTIFICATION

The target characterization parameters are the excitation in-
variant coefficients of the linear homogeneous difference equation
which is satisfied by scattered data from the target. Equivalently
one could say that the characterization parameters are the excitation
invariant complex natural resonances of the target or that the target
is characterized by the excitation invariant difference equation.
The target is also characterized by the <u>excitation dependent</u> residues
in (6) and (7). Use of the residues however would require much larger
storage libraries and a pattern recognition-type learning procedure.
We have consistently advocated a procedure which does <u>not</u> require
parameter extraction from an unknown (source) waveform response.

Let $f_i^{(t)}$ be samples of the response from an unknown target and
$f_j^{(c)}$ be a calculated waveform. First, the calculated waveform is
obtained using (43) which for general m is

$$f_{N+m-y}^{(c)} = -\sum_{\substack{n=0 \\ n \neq y}}^{N} f_{N+m-n}^{(t)} \frac{a_n}{a_y} . \tag{44}$$

$$m = 0, 1, \ldots M.$$

Thus a calculated waveform is obtained using the coefficients of a
known waveform (from the characterization library) and samples of
an unknown waveform. This is prediction. One can now calculate

$$x = 1 - \frac{\sum_{i=0}^{M} (f_{N+i}^{(t)} - f_{N+i}^{(c)})^2}{\sum_{i=0}^{M} (f_{N+i}^{(t)})^2 + (f_{N+i}^{(c)})^2} \tag{45}$$

which is unity minus the normalized squared error between the test
and calculated waveforms for the fixed value of the sampling interval.
The characteristic equation associated with (20) is

33

$$\sum_{n=0}^{N} a_n s^{N-n} = 0, \tag{46}$$

the roots of which are

$$s_i = e^{\gamma_i \Delta t}, \quad i=0,\ldots N. \tag{47}$$

Thus the complex natural resonances are

$$\gamma_i = \frac{1}{\Delta t} \ln(s_i). \tag{48}$$

Equating (46) and a factored form of (46)

$$\sum_{n=0}^{N} a_n s^{N-n} = a_0 \prod_{i=1}^{N} (s+e^{\gamma_i \Delta t}), \tag{49}$$

yields how the coefficients must change with Δt. Finally

$$\rho'' = \sum_{\Delta t} 1 - x(\Delta t), \tag{50}$$

is the identification function. If the test waveform is from the target whose coefficients have been used then values of ρ'' near unity are obtained. Low values of ρ'' indicate a mismatch between the test waveform and target coefficients.

There are of course a number of other methods whereby the parameters discussed above might be used in identification. However, the prediction-correlation shown has performed satisfactorily. For our present purpose the major question is the feasibility of obtaining reasonably stable parameters using data associated with substructure features but not resonances of the target. The actual processing results obtained for pulse response of aircraft via (34) are discussed in a later section of this report.

34

EIGENANALYSIS APPLIED TO MEASURED DATA

Another report on this contract[24] describes methods of obtaining measured spectral and temporal scattering data in some detail. Basically, sampled frequency domain data (magnitude and phase) were measured in two spectral regions; 2.2-4.0 GHz, and 4.0-7.6 GHz for several aircraft models and a pencil-type cavity structure. Each spectral band was spanned by 201 evenly spaced points (200 intervals). Although data from both frequency bands were reported on Reference 24, eigenanalysis was only performed on the 2.2-4.0 GHz data. Time did not permit more than a cursory examination of the higher frequency results.

In previous work on identification at this Laboratory, transient time waveforms were simply obtained from ten frequency harmonically related data. Using higher and more realistic frequencies on this contract necessitated a new technique for obtaining a suitable time domain waveform. The approach employed was to consider the 2.2-4.0 GHz data to be modulated, i.e., effective demodulation of the data from -1.8 to 1.8 GHz and conversion to the time domain via Fourier Series yielded what was considered to be the "envelope" of a short pulse return. These time domain pulse returns are given in the data report[24] and discussed there. In this report the time responses are considered as the data bank to which the eigenanalysis method was applied.

One additional note on the data processing is made. After the frequency domain data were shifted down to be centered at zero frequency a filter, specifically a cos α window, was applied.

The cos α window can be expressed as

$$w(n) = \cos \alpha \left[\frac{n}{N} \pi \right], \quad n = -\frac{N}{2}, \ldots, -1, 0, 1, \ldots, \frac{N}{2} \tag{51}$$

35

The value of α in (51) can be an integer[23], but in our application the value of $\alpha = 25/46$ was used.

Method

Equation (20) given earlier views the general process in terms of the difference equation for a constant sample interval. More detail must be given at this time as a slightly different procedure was used to form the data matrix referred to as (F) in Equation (22). Rewriting (20) as a function of time

$$\sum_{n=0}^{N} f(t_N + m\ t - n\ t)a_n = \epsilon_m \qquad (52)$$

$$; m=0,1,\ldots M; \ (M+1) \geq (N+1).$$

It is seen that as long as the time increment, Δt, multiplying n in (52) is constant in all equations, the difference equation method holds. The Δt multiplying m need not be equal to the Δt multiplying n. The situation can be seen in Figure 8. Forcing the two Δt's to be equal is the situation depicted in (8a); no overlapping occurs. In (8b), however, the Δt multiplying m is smaller, the Δt's overlap, and more use can be made of the appropriate part of the waveform. Calling the smallest increment between samples Δt, Equation (52) can be rewritten as
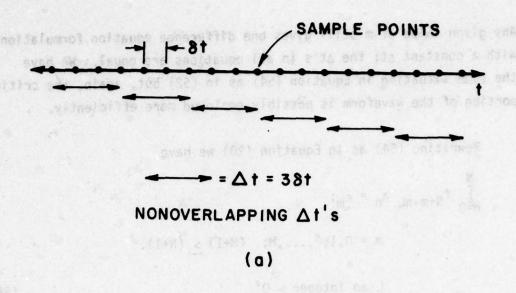
$$\sum_{n=0}^{N} f(t_N + m\delta t - n\Delta t)a_n = \epsilon_m. \qquad (53)$$

Obviously,

$$\Delta t = L \cdot \delta t; \quad L \ \text{an integer} > 0.$$

Then

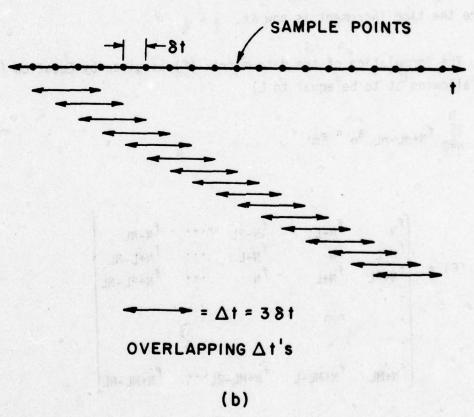$$\sum_{n=0}^{N} f(t_N + m\delta t - nL\delta t)a_n = \epsilon_m. \qquad (54)$$

36

Figure 8. Nonoverlapping (a) and overlapping (b) subintervals.

Any given value of m still gives one difference equation formulation with a constant Δt; the Δt's in all equations are equal. We have the same situation in Equation (54) as in (52) but, again, the critical portion of the waveform is possibly employed more efficiently.

Rewriting (54) as in Equation (20) we have

$$\sum_{n=0}^{N} f_{N+m-nL}\, a_n = \varepsilon_m;$$

$$m = 0,1,2,\ldots,M; \quad (M+1) \geq (N+1).$$

$$L \text{ an integer} > 0 \tag{55}$$

where the time increment is now δt.

The formulation of the data matrix (F) as given by Equation (20) is (allowing Δt to be equal to L)

$$\sum_{n=0}^{N} f_{N+mL-nL}\, a_n = \varepsilon_m, \tag{56}$$

and

$$(F) = \begin{bmatrix} f_N & f_{N-L} & f_{N-2L} & \cdots & f_{N-NL} \\ f_{N+L} & f_N & f_{N-L} & \cdots & f_{N+L-NL} \\ f_{N+2L} & f_{N+L} & f_N & \cdots & f_{N+2L-NL} \\ \cdot & & & & \\ \cdot & & & & \\ \cdot & & & & \\ f_{N+ML} & f_{N+ML-L} & f_{N+ML-2L} & \cdots & f_{N+ML-NL} \end{bmatrix} \tag{57}$$

The formulation for Equation (55) is

$$(F) = \begin{bmatrix} f_N & f_{N-L} & f_{N-2L} & \cdots & f_{N-NL} \\ f_{N+1} & f_{N+1-L} & f_{N+1-2L} & \cdots & f_{N+1-NL} \\ f_{N+2} & f_{N+2-L} & f_{N+2-2L} & \cdots & f_{N+2-NL} \\ \cdot \\ \cdot \\ \cdot \\ f_{N+L} & f_N & f_{N-L} & \cdots & f_{N+L-NL} \\ \cdot \\ \cdot \\ \cdot \\ f_{N+M} & f_{N+M-L} & f_{N+M-2L} & \cdots & f_{N+M-NL} \end{bmatrix} \quad (L+1)+\underline{h} \text{ row} \qquad (58)$$

These two formulations are not simply expressed but the important feature is that the (L+1) row in the second method is the same as the 2nd row in the first method. Again it is seen that more information can possibly be obtained from the important portion of the waveform.

The new procedure exploited in this study was the use of information from two data records (i.e., two aspect angles) in forming the data matrix (F). In practice, (F) was actually formed from two submatrices. Consider one target and a time domain curve $F^i(t)$ from each of two aspect angles. Call them F^1 and F^2. Several constraints exist in forming the new data matrix namely; Δt must be the same for both curves, the number of terms in the desired difference equation must be the same for both curves and the number of rows of (F) must be greater than or equal to the number of columns. This last constraint reflects the least square procedure in Equations (23) through (30) with regard to the (M+1) $\geq$ (N+1) condition of Equations (20) and (55). An N term difference equation (F) could be composed of M1 rows of information from F^1 and M2 rows from F^2. As stated above

39

$$(M1+1)+(M2+1) \geq N+1 \tag{59}$$

but note that M1 is not necessarily equal to M2. We now represent
the data matrix for the following difference equation system

$$\sum_{n=0}^{N} F^1_{N+m-nL}\, a_n = \epsilon_m; \quad m=0,1,\ldots,M1$$

$$\sum_{n=0}^{N} F^2_{N+m-nL}\, a_n = \epsilon_m; \quad m=(m1+1),(M1+2),\ldots,(M1+M2+2). \tag{60}$$

as

$$(F) = \begin{bmatrix}
F^1_N & F^1_{N-L} & F^1_{N-2L} & \cdots & F^1_{N-NL} \\
F^1_{N+1} & F^1_{N+1-L} & F^1_{N+1-2L} & \cdots & F^1_{N+1-NL} \\
\cdot \\
\cdot \\
\cdot \\
F^1_{N+M1} & F^1_{N+M1-L} & F^1_{N+M1-2L} & \cdots & F^1_{N+M1-NL} \\
\hline
F^2_N & F^2_{N-L} & F^2_{N-2L} & \cdots & F^2_{N-NL} \\
F^2_{N+1} & F^2_{N+1-L} & F^2_{N+1-2L} & \cdots & F^2_{N+1-NL} \\
F^2_{N+M2} & F^2_{N+M2-L} & F^2_{N+M2-2L} & \cdots & F^2_{N+M2-NL}
\end{bmatrix} \tag{61}$$

The formulation given by (60) is for two data records. In fact,
the method could be applied to an arbitrary number of data records.
The examples given in this report were restricted to two aspect angles.

In applying Equation (60) to our measured radar data, several
parameters had to be varied. They are:

40

1. N, the number of terms in the difference equation.

2. L, the Δt in the difference equation.

3. M1, the number of rows of information from data record F^1.

4. M2, the number of rows of information from data record F^2.

In general, another variable exists. The portion of the wave-form over which the data is sampled can be changed. In this study, this variable was in effect removed. Examination of (58) reveals that the sample corresponding to the earliest point in time is in the upper right hand corner, F_{N-NL}. On the synthesized pulse responses to which this method was applied, F_{N-NL} was always considered to be the maximum point on the waveform. (See discussion on pulse responses in section on substructure resonances.) The sampled "win-dow" of the waveform was always the maximum point and points to the right of it corresponding to longer times. Some variation in the sampled "window" occurred as N and L (or Δt) were changed. As L was increased for a given N, samples corresponding to longer times were included. Increasing N, the number of terms in the difference eq-uation, also forced inclusion of more data points. Increasing M, the number of rows in the data matrix corresponding to a given record also changes the size of the "window". The starting point, however, was always the maximum point on the waveform. It was always included in this study.

As these variables were adjusted the characteristic being observed was the stability of the difference equation coefficients, the a_n, in Equation (60). By stability here we mean invariance to changes. In this application for a given number of terms in the difference equation N, and a fixed Δt, M1 and M2 were varied and the coefficients examined for stability. Obviously, a change in Δt or N will yield

41

totally different sets of coefficients. The actual procedure used
then was to pick a value of N, pick a value of Δt, and allow M1 and M2
to vary.

Results of this application to several waveforms are given in
the next section.

Results

As stated earlier, the goal of this portion of the effort was
considered to be stability of the coefficients for a given number
of terms in the difference equation and a given Δt as more information
was added to the data matrix (F). Again, changing information in
(F) corresponds to adding rows of elements as defined by a given value
of m in Equation (55) for either of the two aspect angles. Equation
(60) defines the process for two aspect angles. It is seen that there
are MM1 rows of data from aspect angle 1 and MM2 rows of data from
aspect angle 2. The following discussion considers NN to be the number
of terms in the difference equation and IDT to be Δt. The "error"
discussed refers to the total squared error as defined by (20), (i.e.,
the smallest eigenvalue), divided by the trace of (R) where (R) was
defined in Equation (25), and the trace of this real symmetric matrix
is the sum of the diagonal elements. This weighting permits a fair
comparison between errors of different size matrices.

Application of this procedure proved time consuming because a
systemic procedure was not developed for this test. Searching for
stable coefficients initially involved lengthy computer printouts
and visual examination. Figure 9 shows a semi-automated method where
the coefficient values are plotted as functions of their coefficient
numbers. In fact, the computer program has the capability of pro-
ducing these plots on a CRT screen. This greatly aids examination
of the output data.

42

Figure 9 shows difference equation coefficients plotted when the procedure was applied to the time waveforms of Figure 10. (A pencil shape target with a vertical tail stabilizer as described in Reference 24.) As shown, seven coefficients were sought with IDT=4. Note that as MM1 and MM2 are varied (the size of the data matrix changed), the coefficients vary somewhat, i.e., are not stable. Actually, variations were larger than this plot indicates. Figure 9 shows only those cases where the first coefficient was positive. Figure 11 shows the coefficients plotted with six terms in the difference equation and IDT=4 for the same pulse response. Again, stability is not indicated. The case of seven terms in the difference equation and IDT=3 is shown in Figure 12. For these ten values of MM1 and MM2 stability is clearly achieved. In fact, there were more than ten cases which would have shown this stability. Figure 12 also reveals, however, that the first coefficient is very near zero. This indicated that perhaps only six terms are actually needed in the difference equation. Indeed Figure 13 for NN=6 and IDT=3 indicates stability comparable to Figure 12 with no near-zero term. The resulting difference equation indicated by Figure 13 which best fit the two curves of Figure 10 is

$$.182\ F^i(t-\Delta)+.0975F^i(t-2\Delta t)-.0255F^i(t-3\Delta t)$$

$$+\ .495F^i(t-4\Delta t)-.722F^i(t-5\Delta t)+.354F^i(t-6\Delta t)\ =\ 0 \qquad (62)$$

where

$$\Delta t\ =\ 3\cdot\delta\ =\ 3\times0.139\ =\ .417\ ns$$

.139 ns = spacing between time samples

i=1,2 refers to the two data sets.

43

NN= 6   IDT= 3

	MM1	MM2	ERROR	
☉	9	5	3.318	$\times 10^{-7}$
△	9	6	4.553	$\times 10^{-7}$
+	9	7	5.070	$\times 10^{-7}$
✕	9	8	4.984	$\times 10^{-7}$
◇	9	9	7.884	$\times 10^{-7}$
♠	10	5	3.226	$\times 10^{-7}$
✻	10	6	4.449	$\times 10^{-7}$
Z	10	7	5.043	$\times 10^{-7}$
Y	10	8	4.917	$\times 10^{-7}$
✖	10	9	8.639	$\times 10^{-7}$

Figure 13. Difference equation coefficients as a function of
equations from two aspects.

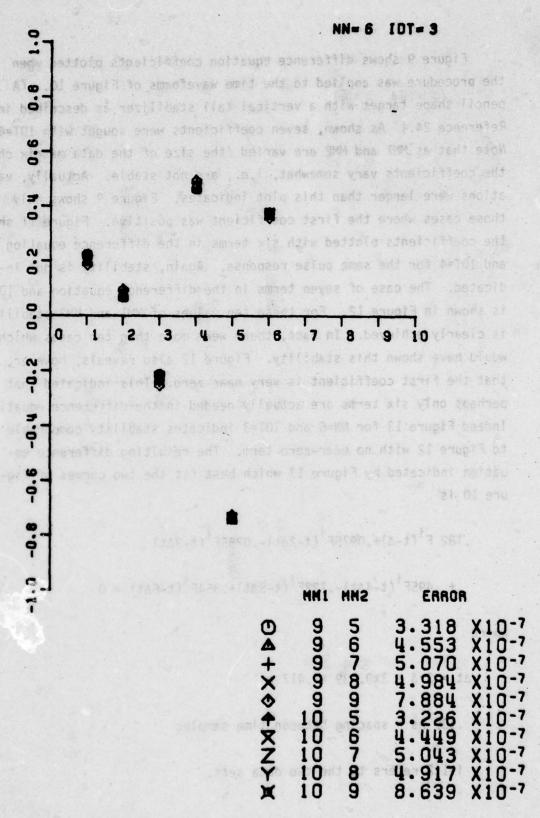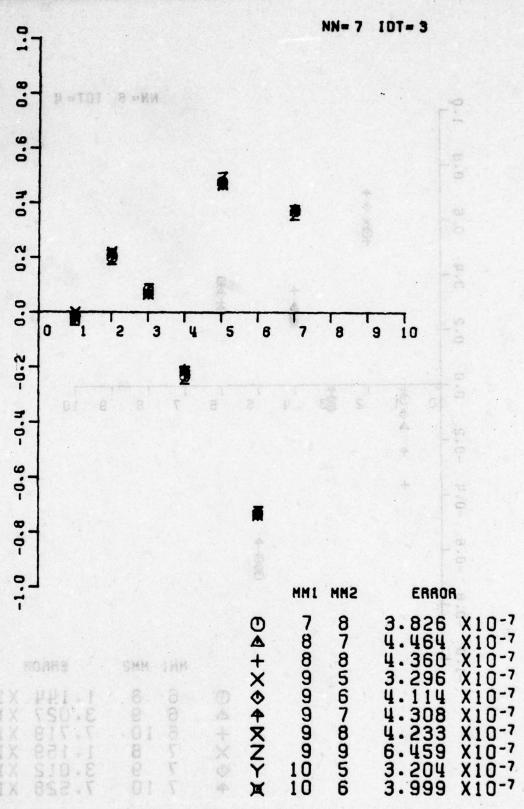|	MM1	MM2	ERROR
⊕	7	8	3.826×10^{-7}
△	8	7	4.464×10^{-7}
+	8	8	4.360×10^{-7}
✕	9	5	3.296×10^{-7}
◇	9	6	4.114×10^{-7}
♠	9	7	4.308×10^{-7}
⊠	9	8	4.233×10^{-7}
Z	9	9	6.459×10^{-7}
Y	10	5	3.204×10^{-7}
✖	10	6	3.999×10^{-7}

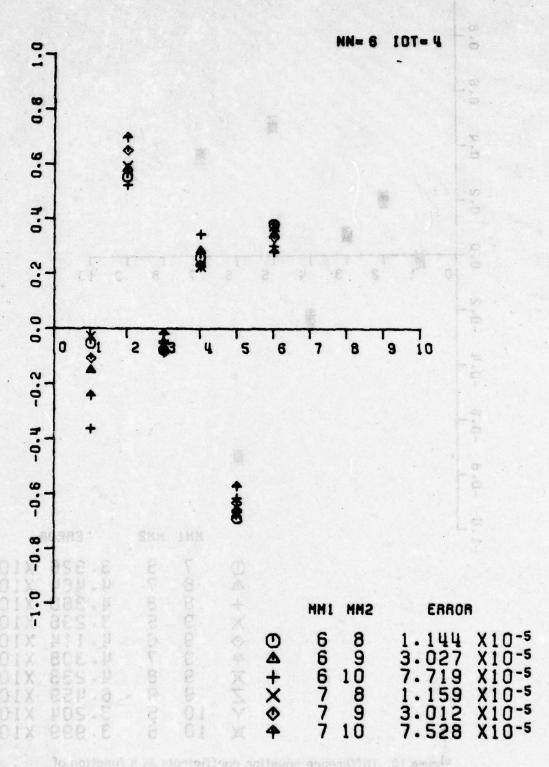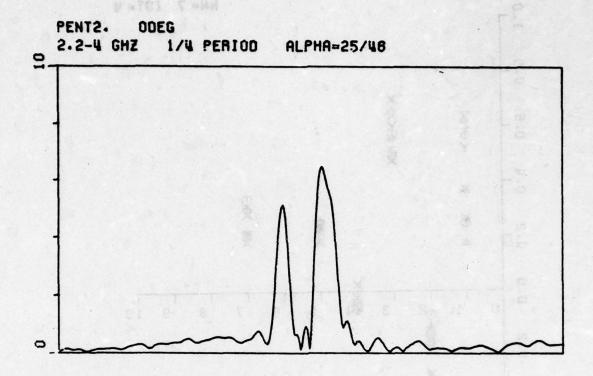Figure 12. Difference equation coefficients as a function of
equations from two aspects.

45

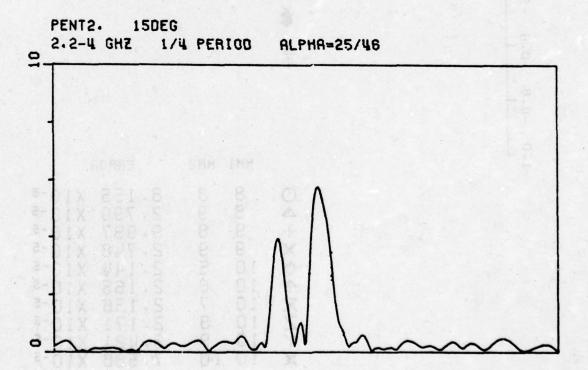Figure 11. Difference equation coefficients as a function of
equations from two aspects.

46

PENT2.   00EG
2.2-4 GHZ   1/4 PERIOD   ALPHA=25/46

PENT2.   15DEG
2.2-4 GHZ   1/4 PERIOD   ALPHA=25/46
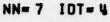
Figure 10. Pulse responses of pencil target 2 inch tail stabilizer.

47

	MM1	MM2	ERROR	
☉	8	8	8.155	$\times 10^{-6}$
△	8	9	2.790	$\times 10^{-5}$
+	9	8	9.997	$\times 10^{-6}$
×	9	9	2.748	$\times 10^{-5}$
◇	10	5	2.144	$\times 10^{-5}$
♠	10	6	2.165	$\times 10^{-5}$
✗	10	7	2.136	$\times 10^{-5}$
Z	10	8	2.171	$\times 10^{-5}$
Y	10	9	3.421	$\times 10^{-5}$
✶	10	10	7.588	$\times 10^{-5}$

Figure 9. Difference equation coefficients as a function of
equations from two aspects.

48

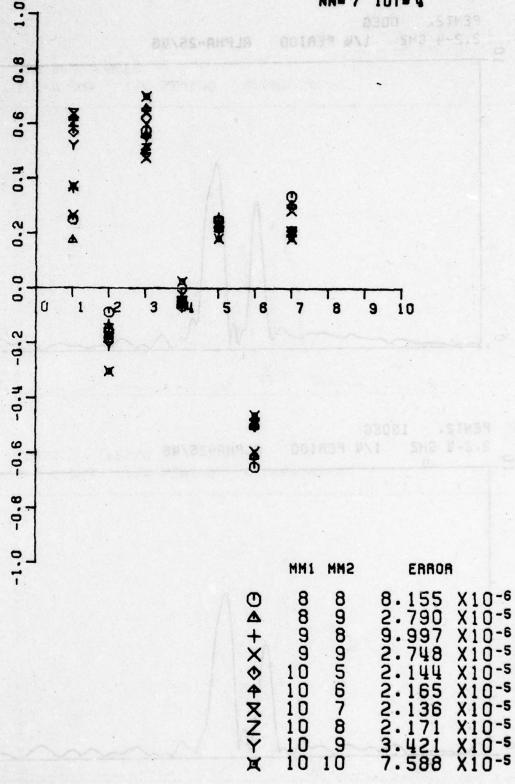This procedure has been applied to several other waveforms but it is interesting here to examine the waveforms of Figure 14. These waveforms correspond to the same pent shaped target on Figure 10 with the exception that the vertical tail fin is slightly longer. Figure 15 shows a stable set of coefficients with five terms and IDT=4. Figure 16 shows a slightly better fit with regard to the total squared error. The difference equation for the target of Figure 14 would be

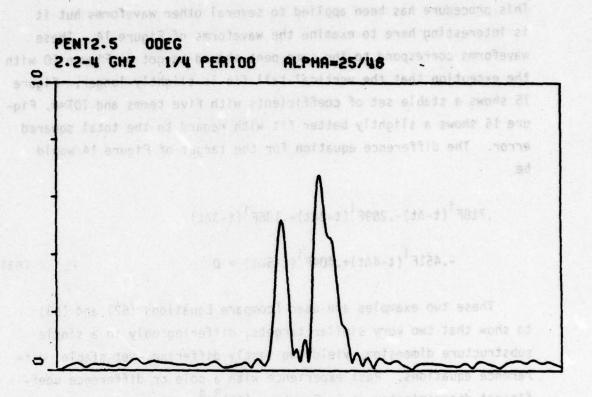$$.718F^i(t-\Delta t)-.289F^i(t-2\Delta t)-.186F^i(t-3\Delta t)$$

$$-.451F^i(t-4\Delta t)+.404F^i(t-5\Delta t) = 0 \qquad (63)$$

These two examples are used (compare Equations (62) and (63) to show that two very similar targets, differing only in a single substructure dimension, yield two vastly differing, yet stable, difference equations. Past experience with a pole or difference coefficient discriminator as in Equation (45)[3,4] indicates that discrimination can be achieved using these coefficients.

DISCUSSION AND CONCLUSIONS

The early sections of this report were devoted to a summary of a basic method of target identification developed over the course of several contracts. These developments are translated here to a set of conclusions addressed specifically to modern fighter aircraft.

1. Scattering data in the spectral range of 2.0 to 24.0 MHz contain the most basic information concerning the overall size and shape of the aircraft.

PENT2.5   00EG
2.2-4 GHZ   1/4 PERIOD   ALPHA=25/46

PENT2.5   15DEG
2.2-4 GHZ   1/4 PERIOD   ALPHA=25/46
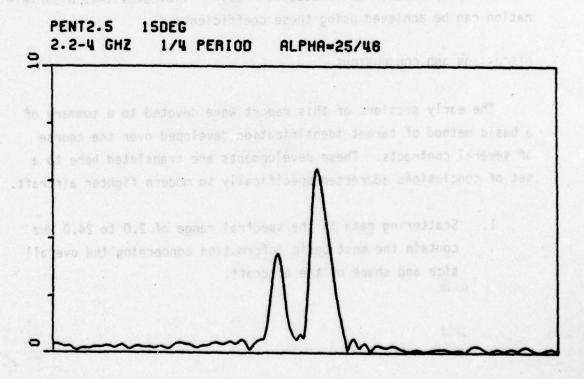
Figure 14. Pulse responses of pencil target 2.5 inch tail stabilizer.

	MM1	MM2	ERROR	
☉	9	7	1.675	X10⁻⁵
△	9	8	2.464	X10⁻⁵
+	9	9	2.712	X10⁻⁵
X	9	10	8.303	X10⁻⁵
◇	10	5	8.840	X10⁻⁶
✦	10	6	1.051	X10⁻⁵
⊠	10	7	1.685	X10⁻⁵
Z	10	8	2.579	X10⁻⁵
Y	10	9	2.762	X10⁻⁵
⋈	10	10	8.094	X10⁻⁵
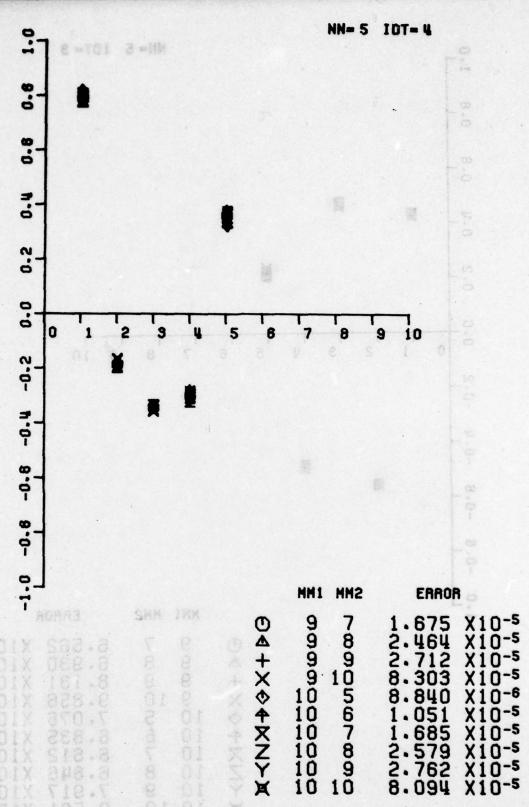
Figure 15. Difference equation coefficients as a function of
equations from two aspects.

51

	MM1	MM2	ERROR
☉	9	7	6.562×10^{-6}
△	9	8	6.930×10^{-6}
+	9	9	8.131×10^{-6}
X	9	10	9.856×10^{-6}
◇	10	5	7.076×10^{-6}
✦	10	6	6.835×10^{-6}
✕	10	7	6.612×10^{-6}
Z	10	8	6.846×10^{-6}
Y	10	9	7.917×10^{-6}
✕	10	10	9.561×10^{-6}
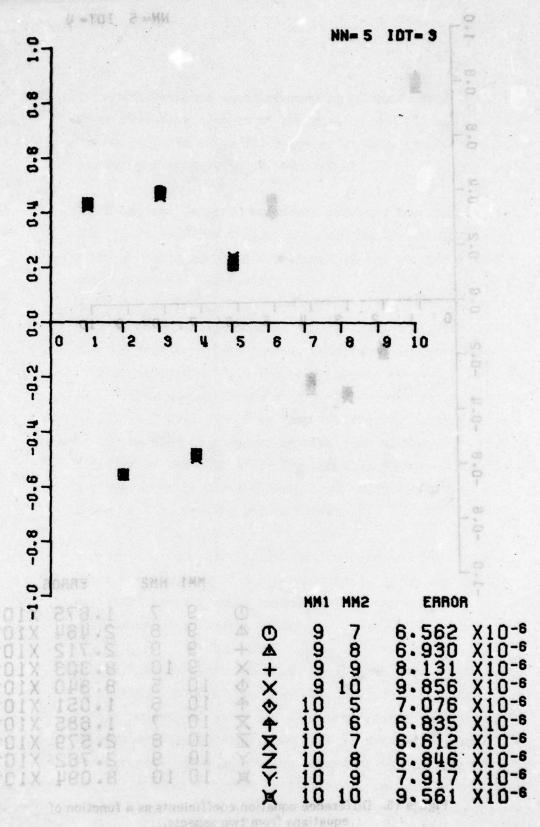
Figure 16. Difference equation coefficients as a function of
equations from two aspects.

52

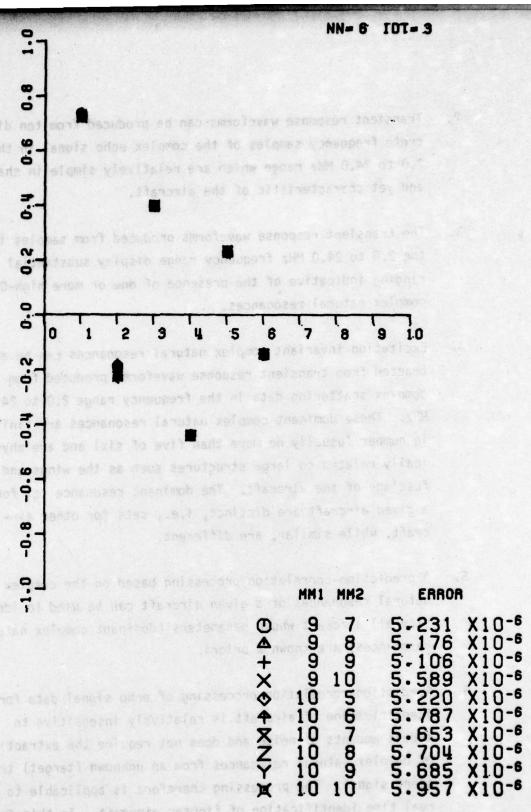|	MM1	MM2	ERROR	
⊙	9	7	5.231	$\times 10^{-6}$
△	9	8	5.176	$\times 10^{-6}$
+	9	9	5.106	$\times 10^{-6}$
X	9	10	5.589	$\times 10^{-6}$
◇	10	5	5.220	$\times 10^{-6}$
✦	10	6	5.787	$\times 10^{-6}$
⊠	10	7	5.653	$\times 10^{-6}$
Z	10	8	5.704	$\times 10^{-6}$
Y	10	9	5.685	$\times 10^{-6}$
⋈	10	10	5.957	$\times 10^{-6}$

Figure 17. Difference equation coefficients as a function of equations from two aspects.

53

2. Transient response waveforms can be produced from ten discrete frequency samples of the complex echo signal in the 2.0 to 24.0 MHz range which are relatively simple in shape and yet characteristic of the aircraft.

3. The transient response waveforms produced from samples in the 2.0 to 24.0 MHz frequency range display substantial ringing indicative of the presence of one or more high-Q complex natural resonances.

4. Excitation invariant complex natural resonances can be extracted from transient response waveforms produced from complex scattering data in the frequency range 2.0 to 24.0 MHz. These dominant complex natural resonances are finite in number (usually no more than five of six) and are physically related to large structures such as the wings and fuselage of the aircraft. The dominant resonance set for a given aircraft are distinct, i.e., sets for other aircraft, while similar, are different.

5. A prediction-correlation processing based on the complex natural resonances of a given aircraft can be used to identify all aircraft whose parameters (dominant complex natural resonances) are known a priori.

6. Prediction-correlation processing of echo signal data for identification of aircraft is relatively insensitive to modest amounts of noise and does not require the extraction of complex natural resonances from an unknown (target) transient signal. The processing therefore is applicable to real time identification of fighter aircraft. In this frequency range minor substructure changes of the aircraft will not negate the identification.

54

Based on the above one can conclude that the identification of modern fighter aircraft is in-hand provided that discrete samples of the complex echo signal spanning the frequency range 2.0 to 24.0 MHz can be obtained. Obviously this identification method is not a retrofit adjustment of existing radar systems. It is stressed, however, that the above requirements for the radar are specifically dictated by the identification task. Stated another way, given complex echo data harmonically spanning the 2.0 to 24.0 MHz frequency band modern fighter aircraft can be identified.

A major task of the present contracts was to determine if modern fighter aircraft could be identified using similar methods if the only available complex echo data were from a significantly higher frequency band, i.e., frequencies above 24 MHz. From a complex natural resonance viewpoint the logical such substructure resonances are those possibly associated with the stabilizer resonances in the 30.0 MHz to 56.0 MHz range and cavity resonances nearer the upper end of the band. Neither calculated nor measured complex echo data are available for fighter aircraft in the 30.0 MHz to 100 MHz frequency region. Furthermore, existing experimental facilities which measure complex echo data at harmonics of some given fundamental frequency are not useful because the frequency increment is too large. To obtain the requisite scattering data several tasks were completed.

7. Preliminary hand-operated stepped frequency complex echo measurements were made in the 30 MHz to 50 MHz region using 1/72 scale models of the F-104, F-4 and MIG-21 aircraft. Frequency increment for these data was 5.0 MHz and a bistatic angle of 30° and vertical (perpendicular to the plane of flight) polarization were used. The measurements were made over a range of aspect angles in the plane of flight. Background subtraction at each discrete frequency was used.

8. From the measured echo data contour plots of the magnitude of the echo signal for frequencies from 30.0 to 50.0 MHz and aspect angles from 0° to 180° were prepared.* Both the preliminary measured data and the contour maps indicated that 30.0 MHz to 56.0 MHz was the frequency region where stabilizer resonances were probable.

9. An automated stepped-frequency measurement range was instrumented. The facility is capable of rapidly measuring and calibrating complex echo signals at stepped frequencies from (model frequencies) 1.0 GHz to 12.0 GHz. The system has a variable bistatic angle and a variable frequency increment between the measured stepped frequencies. Vector background subtraction is used at each measured frequency. Accuracy of the measurements is estimated as ± 1 dB in amplitude and $\pm 10°$ in phase at each frequency.

10. Complex echo signal data in the frequency range 30.0 MHz to 56.0 MHz were measured for six aircraft (F-104, F-4, F15, MIG-21, F-104N, F-105) and one pencil-type shape with an adjustable cavity length. Certain measurements were also made in the frequency range from 56.0 MHz to 106 MHz. Vertical polarization (perpendicular to the plane of flight) were used for transmitter and receiver.

11. Pulse response waveforms with sufficient resolution to isolate substructure features of the aircraft and pencil targets were produced from the stepped frequency data.**

---

*The contour maps were presented in a Quarterly letter dated 13 September 1977.

**The measured data and detailed descriptions of the targets are given in Reference 24. The pulse response waveforms are also given in Reference 24.

As stated in the footnote, a much more detailed discussion of the measurement system, the measured data, the simulated pulse response waveforms and the targets is given in a data report[24]. We concentrate here, however, on certain conclusions most pertinent to the aircraft identification problem.

12. In the frequency range from 30.0 MHz to 56.0 MHz for vertical polarization of transmitter and receiver, the dominant contributor to the echo signal from modern fighter aircraft is the vertical tail stabilizer. For the pencil target at frequencies above 56.0 MHz where the rectangular cavity is above cutoff, the cavity and the position of a short within the cavity are clearly visable in the echo signal.

13. Pulse response waveforms from aircraft simulated from measured complex echo signal measurements in the 30.0 MHz to 56.0 MHz range did not demonstrate the stabilizer assembly has a high-Q complex natural resonance in this frequency range. A similar conclusion can be drawn regarding the cavity at frequencies from 56.0 MHz to 106.0 MHz but is more tentative because the measured data were less extensive.

14. In most cases, the dominance of the vertical stabilizer manifested itself in the pulse responses as a single pulse in the response waveform for a wide variation of aspect angles.

The fact that the stabilizer assembly on fighter aircraft does not have a substructure high-Q complex natural resonance in the frequency range 30.0 MHz to 56.0 MHz was unexpected, and at some variance to earlier pulse responses obtained from echo signals at frequencies below 24.0 MHz. A completely satisfactory explanation of why the tail stabilizer does not have a high-Q type natural resonance in this frequency range cannot be given at this time.

57

15. A method for combining sampled data records of pulse response waveforms from an arbitrary number of target aspects has been developed. As a result it is possible to find that single homogeneous difference equation which best satisfies the transient records of a target for a variety of aspects.

16. It has been demonstrated that an eigenanalysis solution for the coefficients of a linear homogeneous difference equation is more versatile than Prony's method in that no a priori assumptions concerning any of the coefficients is necessary.

The fact that only a single isolated pulse is seen in the transient response of aircraft as simulated from complex echo data in the 30.0 MHz to 56.0 MHz range does not necessarily preclude use of predictor-correlation processing for identification of the aircraft. A difference equation processing can be applied to the tail (portions occuring later in time than the peak) of the pulse response related to the stabilizer. A similar comment can be made concerning the tail of the pencil target. In this regard one can just as easily work with the envelope of the pulse response since it is not anticipated that the complex natural resonances deduced from the coefficients have any physical significance. A physical significance for the coefficient is a convenient but not necessary condition for identification of the target.

17. It has been demonstrated that a set of excitation invariant difference coefficients can be found for the pencil target using pulse responses from various aspects as simulated from echo signal data in the 30.0 MHz to 56 MHz range. It has also been shown that a minor structure change in the vertical stabilizer yields a different set of excitation invariant coefficients. It follows that aircraft with relatively similar stabilizer geometries can still be separately

58

identified. In fact, for the F-105 aircraft model, a set
of difference equation coefficients with stability comparable
to the pen target cases has been found.

Exploitation of the developed measurement facility and processing
of data obtained from this facility has been consistent with the time
and funds of the contract. Fundamental questions concerning the use
of frequencies above 24 MHz for the identification of modern fighter
aircraft have been answered. Certain apparent misconceptions con-
cerning complex natural resonances of substructure of the aircraft
in the frequency range 30.0 MHz to 56.0 MHz have been corrected. Fi-
nally a scheme of identification of fighter aircraft using frequencies
in the 30.0 MHz to 56.0 MHz range has been postulated and certain
requisites of the scheme demonstrated.

It is also apparent that processing tests of measured data already
obtained have been far from exhausted and that many new measurements
and tests have been suggested by the present results. It is strongly
recommended that research programs of this type, which explore the
echo signals of modern fighter aircraft at frequencies above 24 MHz,
be continued.

REFERENCES

1. Kennaugh, E. M. and Cosgriff, R.L., "The Use of Impulse Response in Electromagnetic Scattering Problems," *IRE 1958 National Con. Rec.*, Pt. 1, pp. 72-77.

2. Kennaugh, E. M. and Moffatt, D. L., "Transient and Impulse Response Approximation," *Proc. of the IEEE*, Vol.53, No. 8, August, 1965, pp. 895-901.

3. Moffatt, D. L. and Mains, R. K., "Detection and Discrimination of Radar Targets," *IEEE Trans. on Antennas and Propagation*, Vol. AP-23, No. 3, May 1975.

4. Chuang, C. W. and Moffatt, D. L., "Natural Resonances Via Prony's Method and Target Discrimination," *IEEE Trans. on Aerospace and Electronic Systems*, Vol. 12, No. 5, September 1976.

5. Covington, M. S., "Simplified Calculation of Transient Response," Proc. IEEE, Vol. 53, pp. 287-292, March 1965.

6. Tesche, F. M., "On the Analysis of Scattering and Antenna Problems using Singularity Expansion Techniques," *IEEE Trans. Antennas Propagat.*, Vol. AP-21, pp. 53-62, January 1973.

7. Stratton, J. A., *Electromagnetic Theory*, McGraw-Hill Book Co., Inc., New York, 1941.

8. Moffatt, D. L., "Time Domain Electromagnetic Scattering from Highly Conducting Objects," Ohio State University ElectroScience Laboratory report 2971-2, May 1971. (AFCRL-71-0319) (AD 885883)

9. Lin, Y. T. and Richmond, J. H., "EM Modeling of Aircraft at Low Frequencies," _IEEE Trans. on Antennas and Propagation_, AP-23, No. 1, pp. 53-56, January 1975.

10. Richmond, J. H., "Radiation and Scattering by Thin-Wire Structures in the Complex Frequency Domain," National Aeronautics and Space Administration, NASA CR-2396, May 1974.

11. Hildebrand, F. B., _Introduction to Numerical Analysis_, McGraw-Hill Book Co., Inc., 1956.

12. Moffatt, D. L. and Shubert, K. A., "Natural Resonances Via Rational Approximants," _IEEE Trans. Antennas Propagation_, Vol. AP-25, No. 5, September 1977, pp. 657-660.

13. Berni, A. J., "Target Identification by Natural Resonance Estimation, _IEEE_ Trans. on Aerospace and Electronic Systems, AES-11, pp. 147-154, March 1975.

14. Hodge, D. B., "Spectral and Transient Response of a Circular Disk to Plane Electromagnetic Waves," _IEEE Trans. on Antennas and Propagation_, Vol. AP-19, No. 4, pp. 558-561, July 1971.

15. Hill, D. A., "Electromagnetic Scattering Concepts Applied to the Detection of Targets Near the Ground," Ohio State University ElectroScience Laboratory Report 2971-1, September 1970. (AFCRL-70-0250) (AD 875889)

16. Moffatt, D. L. and Puskar, R. J., "A Subsurface Electromagnetic Pulse Radar," Geophysics, Vol. 41, No. 3, June 1976, pp. 506-518.

61

17. Mains, R. K. and Moffatt, D. L., "Complex Natural Resonances of an Object in Detection and Descrimination," Ohio State University ElectroScience Laboratory, Department of Electrical Engineering, Report 3424-1, June 1974 for Elec. Sup. Div., Laurence G. Hanscom Field, Bedford, Mass.

18. Shubert, K. A., Young, J. D., and Moffatt, D. L., "Synthetic Radar Imagery," IEEE Trans. Antennas Propagation, vol. AP-25, No. 4, July 1977, pp. 477-483.

19. Moffatt, D. L., "Characterization of Subsurface Electromagnetic Soundings," Report 784490-1, May 1977, The Ohio State University ElectroScience Laboratory, Department of Electrical Engineering; prepared under Grant ENG76-04344 for National Science Foundation.

20. "Short Course Notes on Radar Target Identification," The Ohio State University, September 1977.

21. Chuang, C. W. and Moffatt, D. L., "Complex Natural Resonances of Radar Targets Via Prony's Method," Report 3424-3, April 1975, The Ohio State University ElectroScience Laboratory, Department of Electrical Engineering; prepared under Contract F19628-72-C-0203 for Air Force Systems Command, Hanscom Air Force Base. (AFCRL-TR-75-0203)

22. Chuang, C., Moffatt, D., Peters, L., Jr., Shubert, K.A., "Continuation of the Investigation of the Multifrequency Radar Reflectivity of Radar Target Identification," Report 3424-7, March 1977, The Ohio State University ElectroScience Laboratory, Department of Electrical Engineering; prepared under Contract F19628-72-C-0203 for Air Force Systems Command, Hanscom Air Force Base. (RADC-TR-77-115) (A040347)

23. Harris, Frederic J., "On the Use of Windows for Harmonic Analysis with the Discrete Fourier Transform," Proc. of the IEEE, Vol. 66, No. 1, January 1978, pp. 51-83.

24. Shubert, K. A. and Moffatt, D. L., "Swept Frequency Scattering Measurements of Aircraft," Report 784677-1, January 1979, The Ohio State University ElectroScience Laboratory, Department of Electrical Engineering; prepared under Contract F19628-77-C-0123 for Electronic Systems Division, Hanscom Air Force Base, Massachusetts.

25. Joint Services Electronics Program, Annual Report 710816-1, December 1978, The Ohio State University ElectroScience Laboratory, Department of Electrical Engineering; prepared under Contract N00014-78-C-0049 for Office of Naval Research.

26. "Characterization of Subsurface Electromagnetic Soundings," Report 784490-2, January 1979, The Ohio State University ElectroScience Laboratory, Department of Electrical Engineering; prepared under Grant NEG76-04334 for National Science Foundation.

MISSION
of
Rome Air Development Center

RADC plans and executes research, development, test and selected acquisition programs in support of Command, Control Communications and Intelligence (C^3I) activities. Technical and engineering support within areas of technical competence is provided to ESD Program Offices (POs) and other ESD elements. The principal technical mission areas are communications, electromagnetic guidance and control, surveillance of ground and aerospace objects, intelligence data collection and handling, information system technology, ionospheric propagation, solid state sciences, microwave physics and electronic reliability, maintainability and compatibility.